

NPS ARCHIVE
1961
HULL, A.

A METHOD OF FORECASTING
THE FORMATION OF 500-MILLIBAR BLOCKS
USING STATISTICAL PARAMETERS

ARTHUR N. HULL

LIBRARY
U.S. NAVAL POSTGRADUATE SCHOOL
MONTEREY, CALIFORNIA

A METHOD OF FORECASTING THE FORMATION OF 500-
MILLIBAR BLOCKS USING STATISTICAL PARAMETERS.

* * * * *

Arthur N. Hull

A METHOD OF FORECASTING THE FORMATION OF 500-
MILLIBAR BLOCKS USING STATISTICAL PARAMETERS.

by

Arthur N. Hull

This work is accepted as fulfilling
the thesis requirements for the degree of

MASTER OF SCIENCE

IN

METEOROLOGY

from the

United States Naval Postgraduate School

A METHOD OF FORECASTING THE FORMATION OF 500-
MILLIBAR BLOCKS USING STATISTICAL PARAMETERS.

by

Arthur N. Hull

//

Submitted in partial fulfillment of
the requirements for the degree of

MASTER OF SCIENCE
IN
METEOROLOGY

United States Naval Postgraduate School
Monterey, California

1 9 6 1

TABLE OF CONTENTS

Section	Title	Page
1.	Introduction	1
2.	Data Collection	2
3.	Method of Computation	3
4.	Evaluation of Computations	4
5.	The Forecast Procedure	12
6.	Results and Conclusions	14
7.	Bibliography	25
Appendix I	Height anomalies for 15 cases of Sub-Icelandic Blocks	26
Appendix II	Height anomalies for 15 cases of non-blocks in Sub-Icelandic area	28
Appendix III	Test data; height anomalies for 15 block cases, miscellaneous areas	30
Appendix IV	Test data; height anomalies for 15 cases of non-blocks, miscellaneous areas	36

LIST OF ILLUSTRATIONS

Figure		Page
1.	Weather plotting map illustrating stations and station indicators used in development	2
2.	Comparison of spacing of station indicators used in both development phase and forecast phase.	13
3.	Graph of relative confidence values for A_6V_6 .	17
4.	Graph of relative confidence values for B_6V_6	18
5.	Graph of relative confidence values for C_5Q_5 .	19
6.	Graph of relative confidence values for C_5R_5 .	20
7.	Graph of relative confidence values for C_5Q_4 .	21
8.	Graph of relative confidence values for A_3S_3 .	22
9.	Graph of relative confidence values for A_3T_3 .	23
10.	The forecast graph with E_1 and E_2 given by equations 8 and 9.	24

LIST OF TABLES

Table		Page
1.	Table of significant height-anomaly correlations with no lag.	7
2.	Table of significant height-anomaly correlations with various lags.	10
3.	Table of significant correlations of 24-hour height tendencies with various lags.	11
4.	Contingency table of forecast results.	15

LIST OF ABBREVIATIONS AND SYMBOLS

A	Station Identifier
B	Station Identifier
C	Station Identifier
C.G.	Center of Gravity
c	Relative confidence value
D	Station Identifier
E_1	First predictor
E_2	Second predictor
F-DAY	Formation day of block
F-6	Six days prior to block formation (similarly for F-5, etc.)
Q	Station identifier
R	Station identifier
S	Station identifier
SSW	Selfridge, Stevenson, and Wood, co-authors of reference [6]
σ	Standard deviation
T	Station identifier
U	Station identifier
V	Station identifier
W	Station identifier
x, y	General terms and subscripts used in formulae development.

Z	500-mb actual height
\bar{Z}	Long-term mean 500-mb height
z	500-mb height anomaly
\bar{z}	mean 500-mb height anomaly

Subscripts

Letters	Refer to station identifiers
Numbers	Refer to days prior to block formation

Example: Z_{A6} - 500-mb actual height at station A on F-6.
 z_{A6} - 500-mb height anomaly at station A on F-6.
 Later in the thesis this notation is shortened to simply A_6 .
 A_{54} - 500-mb height-anomaly tendency at station A between F-5 and F-4

ABSTRACT

An investigation is made of the statistical properties of blocks at the 500-mb level along the latitude belt 50-55N covering 180 degrees of longitude including the block area. From the results obtained a method of computing a 72-hour forecast of block formation is developed.

The author is deeply indebted to Professor Frank L. Martin for his advice and guidance during the progress of this investigation. Grateful acknowledgement is also due Professor Richard C. Campbell for his invaluable aid in programming the statistical routine used in the CDC-1604 computer.

1. Introduction

Extended forecasting by statistical means is a field of meteorology relatively untapped yet showing vast promise of success. The most fruitful attempts appear to be in the field of weather-typing as used by Elliott [2] et al, and weather typing by orthogonal functions as used by Malone [4, chapter 28] et al. The one major shortcoming of weather-typing, however, lies in the difficulty of predicting the type to follow.

The most persistent weather type in any one area is the block. Definitions of blocks vary widely but all definitions require a relatively stationary flow pattern for periods ranging from three to more than ten days. Predictability of the formation of a block in any one sector would thus aid weather-typing considerably. It is the purpose of this investigation, therefore, to devise a method of forecasting block-formations at 500 mb using statistical parameters.

Rex [5] thoroughly investigated blocking patterns in the lower and middle troposphere, and correlated anomalies of temperature and precipitation with marked success. In his definition of a block, the flow pattern was required to maintain its identity for a period of at least ten days. Selfridge, Stevenson, and Wood [6], hereafter referred to as SSW, based their findings on the definition used by Serbreny [7,8] that a block must remain in the sector of origin for a

period of at least three days. In this study, all the characteristics of block types described by SSW and Serebreny have been utilized. Blocking-type boundaries are as defined by SSW and Serebreny. This investigation covers the period from six days before the formation of a block, F-6 day, until F-DAY, which is the day the block is actually within the defined type boundaries.

Because of the availability of ocean stations and land stations both upwind and downwind, the Sub-Icelandic block was chosen for use as development data in this investigation. The formation area for the Sub-Icelandic block is contained within the area 50-65N and 10-30W.

2. Data Collection

Eleven stations were selected within the boundaries 50-55N and 10E to 177W in order adequately to cover the area in which it was believed indications of block formation would appear. The stations selected are as indicated in Fig. 1 below.

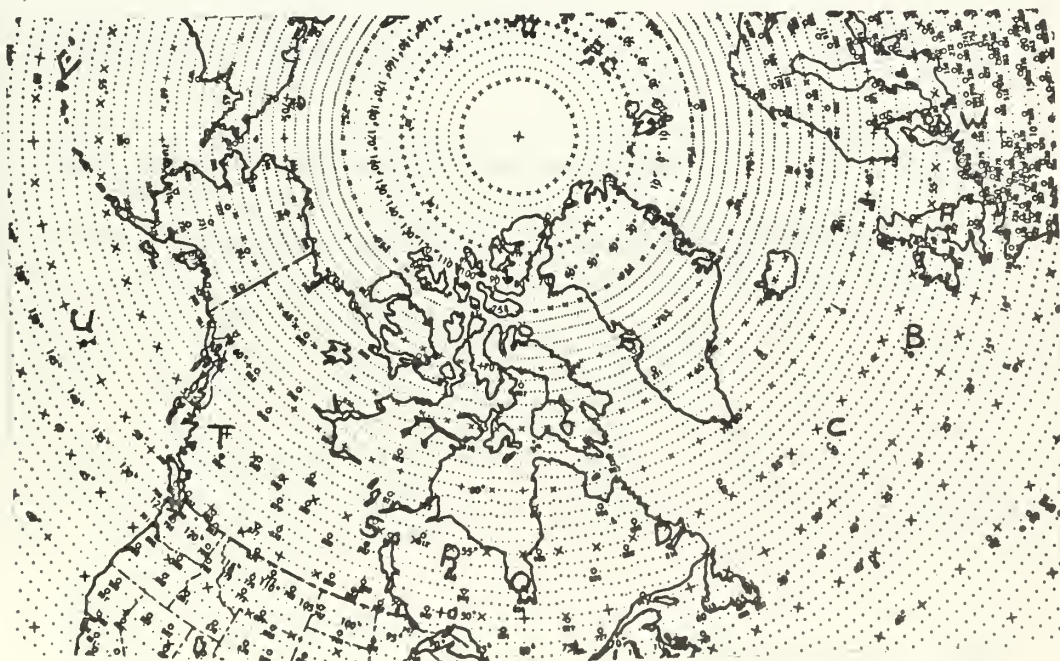


Fig. 1. Weather plotting map illustrating stations and station indicators used in development.

For all fifteen winter cases of Sub-Icelandic blocks listed in the calendar of types in SSW, the actual 500-mb data were collected for the period ranging from F-6 through F-DAY from the Historical Weather Map Series [10].

The mean monthly contours from "Normal 500-mb Charts for the Northern Hemisphere"[11] were used to obtain the 500-mb mean height for each station in the month of each block. In some cases, linear extrapolation was used for computing the means.

From the observed heights and their means, height anomalies were computed. These data were transferred to IBM punch cards. Linear correlation computations between height anomalies were then produced for all eleven stations taken two at a time, and for each day prior to and including F-3.

3. Method of Computation

All computations were made using the CDC-1604 computer.

Data were programmed using the formulae listed below:

$$Z_x - \bar{Z}_x = z_x, \quad (1)$$

$$Z_Y - \bar{Z}_Y = z_Y, \quad (2)$$

$$\bar{Z}_x = \frac{1}{n} \sum z_x, \quad (3)$$

$$\bar{z}_Y = \frac{1}{n} \sum z_Y, \quad (4)$$

$$\sigma_{z_x}^2 = \frac{1}{n} \sum (z_x - \bar{z}_x)^2, \quad (5)$$

$$\sigma_{z_Y}^2 = \frac{1}{n} \sum (z_Y - \bar{z}_Y)^2, \quad (6)$$

$$r_{xy} = \frac{\sum (z_x - \bar{z}_x)(z_Y - \bar{z}_Y)}{n \sigma_{z_x} \sigma_{z_Y}}. \quad (7)$$

In the set of formulae above, $n=15$ is the sample size, z_x is the height anomaly at station x for the specified day before block formation. r_{xy} is a correlation between z_x and z_Y . In most cases correlations for the same day were preferred (Table 1); correlations involving different time lags were also performed (Table 2). In addition, 24-hour height-change values were correlated across the entire network of stations (Table 3). In general, these gave many excellent significant correlations but were not considered to be as useful predictors as the previous two types of correlation coefficients.

In all computations, heights as measured, and anomalies as computed are in tens of feet.

4. Evaluation of Computations

From Hoel [1], assuming that the long-term theoretical correlation of height anomalies between stations is equal to zero, and that the height anomalies are normally distributed, an actual value for the correlation coefficient (based on 15 independent cases) whose magnitude is equal to or greater than 0.473 is significant at the 95% level of

belief. The criteria for the selection of prediction stations were that, in all cases, the correlation coefficients between stations must be greater than 0.473 in magnitude and, furthermore, there must be at least three stations which are mutually and significantly correlated. Trial predictor stations were selected from the list of correlations shown in Table 1.

Since it had been previously determined that a 72-hour forecast would be developed, the correlations for F-2, F-1, and F-DAY were not used in the development.

Graphs of height anomalies were next drawn for each pair of significantly correlated stations associated with block formation. These graphs are shown in Figs. 3 through 9.

Using a table of random numbers [12] , fifteen cases of non-blocks were randomly selected and height anomalies for these cases were plotted on the appropriate graphs for the corresponding day. The regression line for block cases only was plotted on each graph.

A discriminant analysis of the type used by Miller [3] was next performed on each graph. It was discovered, as expected, that the correlation between a station the the block area and one immediately adjacent was uniformly positive, and in no way discriminated between blocks and non-blocks. Of 17 graphs tested, 10 were rejected as having no forecast value.

On the graphs which were retained, subjective analysis of the type used by Thompson [9] was conducted. This consisted of drawing rel-

ative confidence isolines numbered from 0 to 5 on each graph. The "5" isoline encircles clusters of block cases near the regression line, and the "0" line is near the axis of the perpendicular to the regression line. Essentially the areas within the "0" and "5" lines test the hypotheses to reject or accept block formation respectively, while the remaining areas delineate the intermediate critical region. No block case was permitted to correspond to a relative confidence value of less than three. This in effect assigned spacial weights in the critical region.

The critical region was further tested in the following manner:

(1) it is assumed that the events leading up to block formation are sequential in nature and therefore to be equally weighted; and (2) the relative confidence value from each graph is summed for each day, thus assigning equal weight for each graph. The graphs which display these relative confidence isolines are shown in Figs. 3 through 9.

It was noted that some blocking cases which had high relative confidence values on F-6 and F-5 had low values on F-3. Since no combination of pairs of stations gave good correlations on F-4, it was necessary to use a discriminant analysis between F-5 and F-4. Accordingly, the relative confidence values for the four graphs on F-6 and F-5 were summed and termed the first predictor (E_1). Since each day was to be equally weighted, the second predictor (E_2) was formed by summing twice the relative confidence value of the F-4 graph plus the sum of the F-3 graphs. These two predictors for non-block and

Table 1. Table of significant height-anomaly correlations with no lag.

Anomalies Correlated	F-6	F-5	F-4	F-3	F-2	F-1	F-DAY
W A	0.47	0.68	0.56-	0.79	0.87	0.74	0.77
A B	0.66	0.55	0.60	0.55	0.52		
B C	0.68	0.47		0.52		0.53	
C D					0.49		
D Q		0.49					
Q R	0.79	0.69		0.72	0.79	0.74	0.75
R S	0.69	0.85	0.63	0.86	0.77	0.82	0.53
S T				0.56		0.49	
T U		0.55					
U V							
W B							
A C							
B D				-0.51			
C Q	-0.47	-0.63*	-0.49				
D R						0.66	
Q S		0.58		0.58			
R T							
S U	-0.55	-0.66					
T V				-0.62	-0.58	-0.57	
W C							

* - Denotes those correlations used in the forecast procedure

Table 1 (continued)

Anomalies	Correlated	F-6	F-5	F-4	F-3	F-2	F-1	F-DAY
A D								-0.47
B Q				-0.57		-0.49		
C R			-0.59*					
D S							0.48	
Q T								
R U			-0.48					
S V					-0.57	-0.65	-0.48	
W D		-0.52						
A Q								
B R					-0.62	-0.57	-0.49	
C S								
D T		-0.49						
Q U				-0.49				
R V						-0.62		
W Q								
A R					-0.58	-0.50		
B S					-0.65			
C T					0.47			
D U								
Q V								

* - Denotes those correlations used in the forecast procedure

Table 1 (continued)

Anomalies Correlated	F-6	F-5	F-4	F-3	F-2	F-1	F-DAY
W R							
A S				-0.59*			-0.53
B T							
C U							
D V							
W S							
A T				-0.49*			
B U							
C V							
W T				-0.50			-0.48
A U							
B V	-0.70*	-0.67					
W U							
A V	-0.48*						
W V							

* - Denotes those correlations used in the forecast procedure.

Table 2. Table of significant height-anomaly correlations with various lags.

Anomalies Correlated	Correlation Coefficient
$W_2 T_3$	-0.54
$A_3 R_2$	-0.58
$A_3 S_2$	-0.51
$S_2 T_3$	0.65
$A_3 T_2$	-0.49
$C_1 V_6$	-0.63
$A_3 D_5$	-0.47
$W_6 A_5$	0.69
$A_5 D_2$	-0.55
$C_5 Q_4$	-0.83*
$C_5 V_2$	0.55
$D_3 D_2$	0.50
$D_3 Q_4$	0.55
$R_4 S_5$	0.49
$S_5 V_2$	-0.71
$U_3 V_2$	0.52

* - Denotes those correlations used in the forecast procedure

Table 3. Table of significant correlations of 24-hour height tendencies with various lags.

Anomalies Correlated	Correlation Coefficient
B ₁₀ Q ₅₄	0.90
B ₁₀ C ₃₂	-0.50
C ₃₂ Q ₅₄	-0.66
W ₅₄ D ₄₃	-0.60
W ₅₄ S ₃₂	-0.60
B ₂₁ C ₃₂	0.72
B ₁₀ D ₄₃	0.58
D ₄₃ Q ₅₄	0.54
Q ₅₄ S ₃₂	0.63
T ₅₄ U ₃₂	-0.51

block cases were next plotted (Fig. 10). The centers of gravity for block cases and non-block cases were next determined and a line joining these centers of gravity was constructed. The standard deviation for non-blocks was next determined and a distance along the line connecting the two centers of gravity of 1.64 standard deviations from the center of gravity of non-blocks was marked. A line perpendicular to the line joining the centers of gravity was drawn through this point. Assuming the predictor values are normally distributed, non-blocks lying on the block side of this line have less than a 10% chance of occurrence.

5. The Forecast Procedure

As stated earlier, it was assumed that the mechanisms or the series of events correlated are sequential in the case of the Sub-Icelandic block. For the forecast procedure, it was further assumed that this series of sequential correlations holds true for any block and that only a shift in base line is necessary for computation. Therefore, a base line as close as possible to the one used in the Sub-Icelandic block computations has been developed. For simplicity, the latitude line of 50N was selected as the base line. Station locations are as indicated in Fig. 2 below.

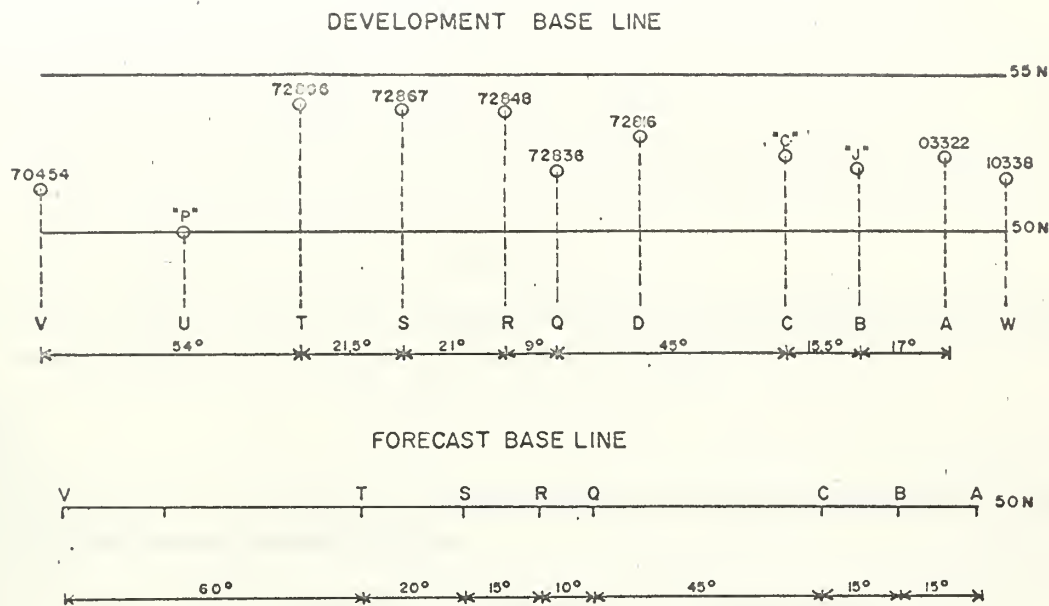


Fig. 2. Comparison of spacing of station indicators used in both development phase and forecast phase.

For any type of block, the longitude of the center of the block-type area as defined by Serebreny [5, 6] and SSW is used as the longitude of station B. The other stations are located east or west of this point as indicated by the "forecast base line" of Fig. 2.

Using the same station identifiers as in the development stage but oriented relative to the new base line, height anomalies are computed for stations A, B, and V for F-6 and stations C, Q, and R for F-5. Relative confidence values are determined from the appropriate graphs and summed for the first predictor,

$$E_1 = c(A_6 V_6) + c(B_6 V_6) + c(C_5 Q_5) + c(C_5 R_5). \quad (8)$$

Height anomalies are then computed for station Q on F-4, and for stations A, S, and T on F-3. Relative confidence values are then obtained from the appropriate graphs and summed according to the formula be-

low to obtain the second predictor

$$E_2 = 2c(C_5Q_4) + c(A_3S_3) + c(A_3T_3). \quad (9)$$

Test data were thus obtained for each of 15 winter cases of blocks and non-blocks in the following areas:

1) three cases each of Bering Sea-Western Alaska blocks, Sub-Aleutian blocks, and Scandanavian-Baltic blocks;

and

2) two cases each of Sub-Icelandic blocks, England-North Sea blocks, and Western Canada blocks.

The results of these computations are indicated in Fig. 10. The data for these computations are compiled in Appendices III and IV.

6. Results and Conclusions

From the space correlations in SSW, the expected frequency of block days in all four sectors which they investigated is 903 block days out of a possible 2168 days. Of these block days, 209 were initial formation days. The remaining block days were rejected from the total, since only initial block days and non-block days were used in testing. The climatological expectancy of block formations thus is 0.142 per day. The climatological expectancy of non-block days is then considered to be $1-0.142=0.858$. From the sample summarized in Table 4, a forecast accuracy of 87 percent and a skill score, based on the climatological expectencies, of 0.73 were obtained.

Table 4. Contingency table of forecast results.

Forecast	Observed	
	Blocks	Non-blocks
Blocks	13	2
Non-blocks	2	13

In conclusion, although few cases were used to derive this forecast procedure, the results indicate that sequential correlations do exist, both upwind and downwind during block formation, that can be utilized to make a 72-hour forecast. It is believed that 1) by increasing the base line to a full 360 degree arc around the latitude belt of 50N, 2) by decreasing the station-to-station interval to a constant 15 degrees of longitude, and 3) by studying many more cases, that sequential correlations will be found to exist that will correctly forecast not only block formation but also block dissipation. It is also within the realm of possibility that the forecast can be extended to a period of greater than 72 hours. It is further believed that such forecasting methods as presented herein may be of great value in determining empirical relationships to be entered as corrections or modifications to the results of numerical prognostic maps as currently being issued.

Figs. 3 - 9 Graphs of relative confidence isolines.
Fig. 10 The forecast graph

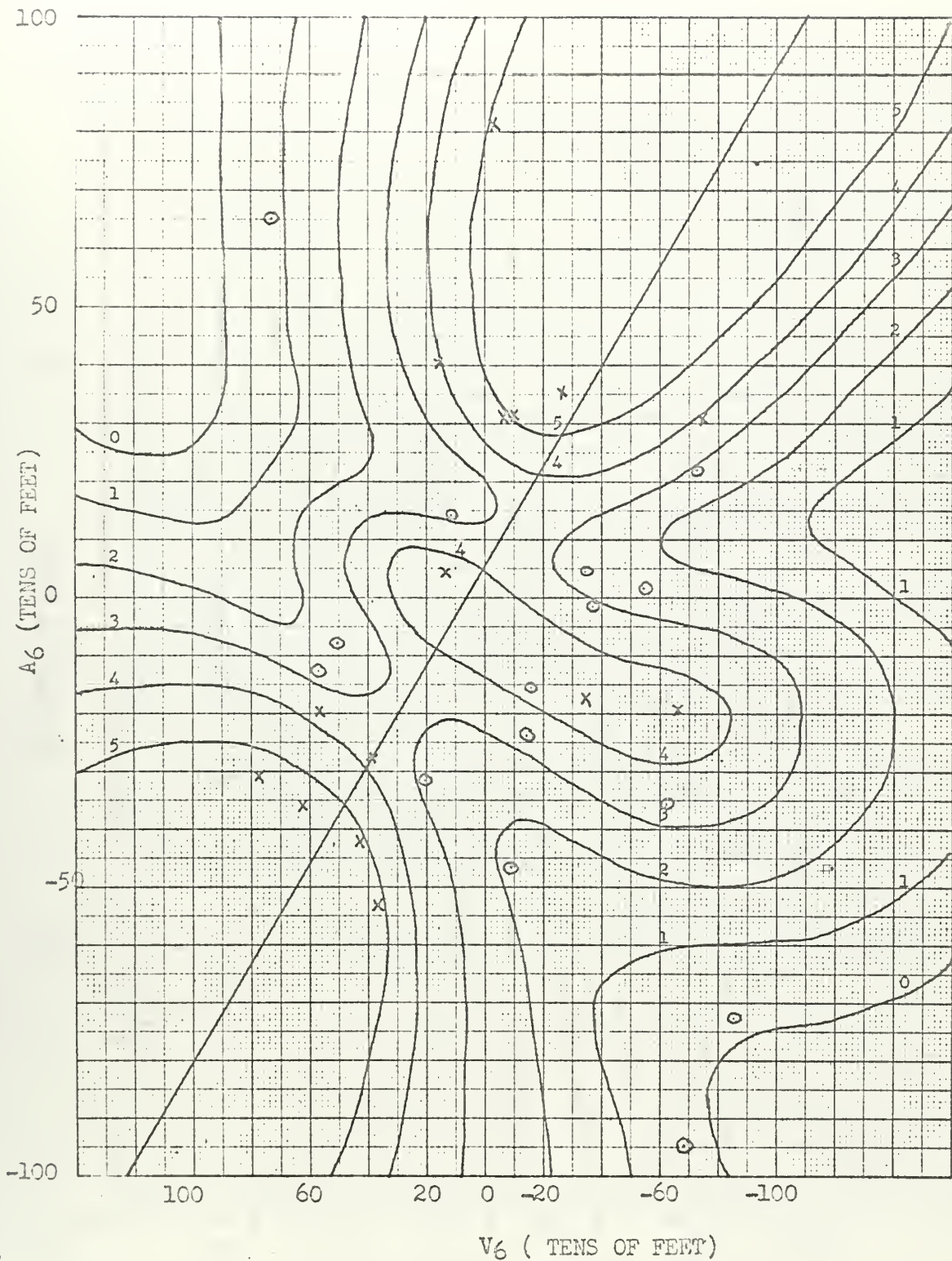


Fig. 3 Graph of relative confidence values for A_6V_6 .

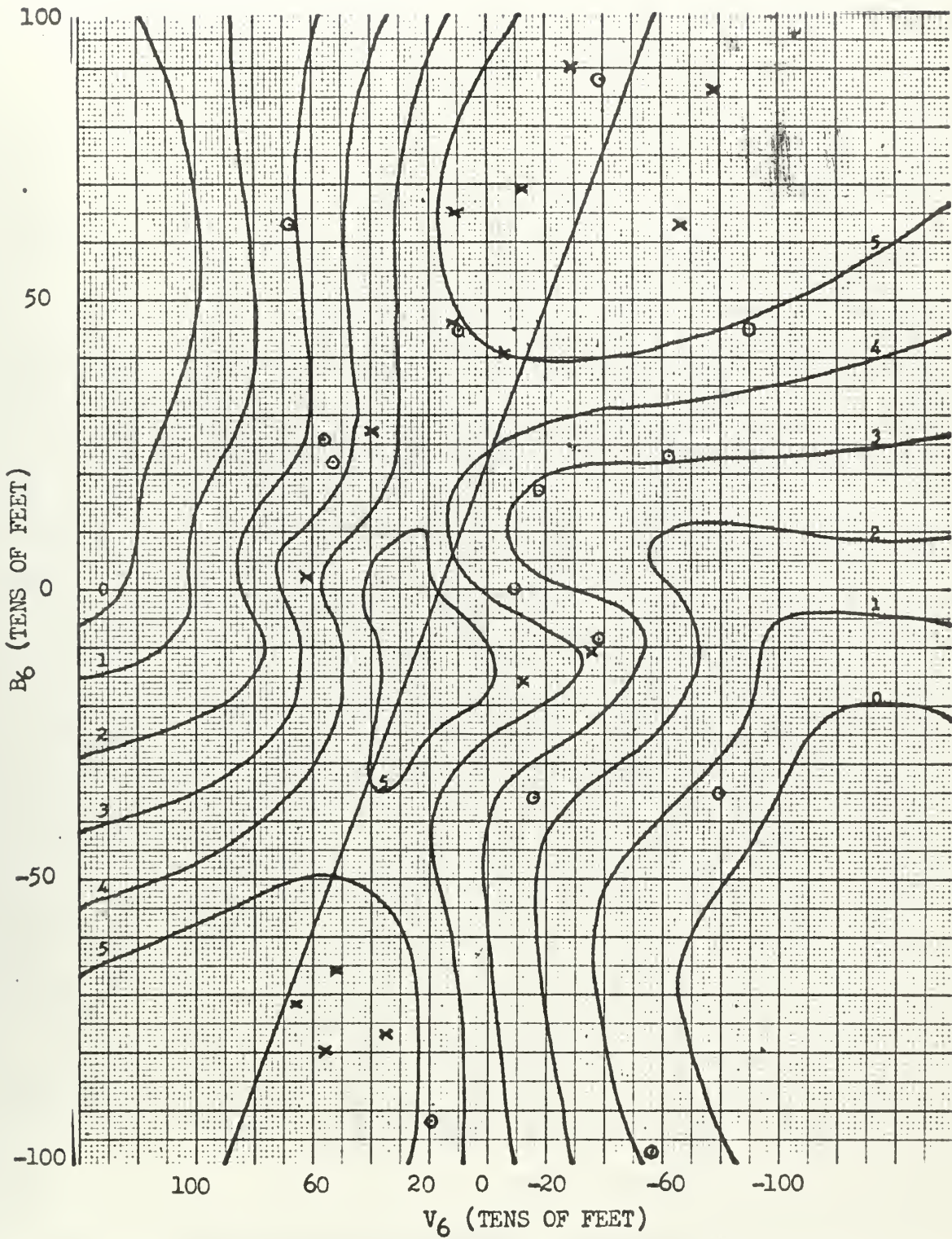


Fig. 4 Graph of relative confidence values for B_6V_6 .

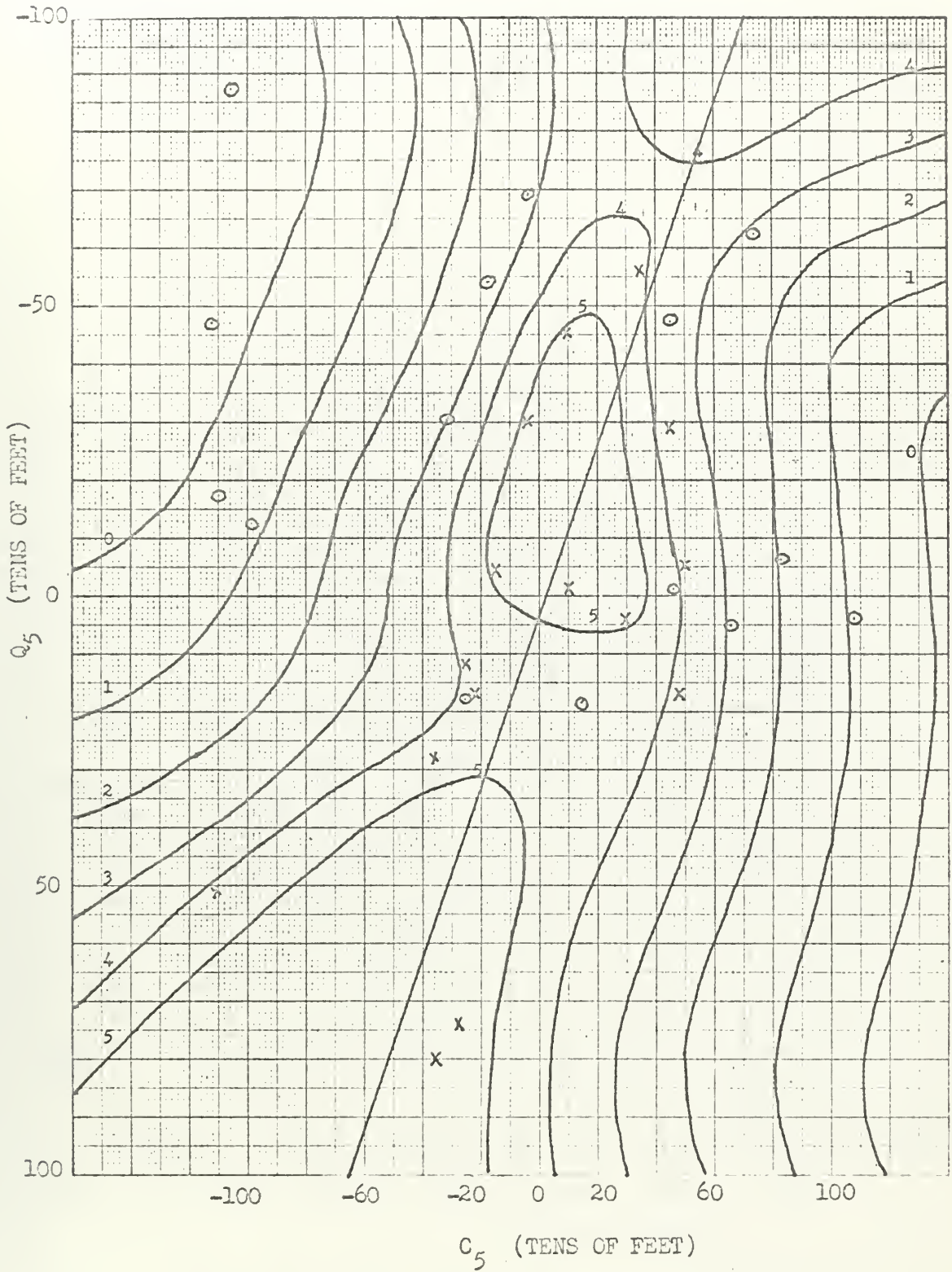


Fig. 5 Graph of relative confidence values for C_5Q_5 .

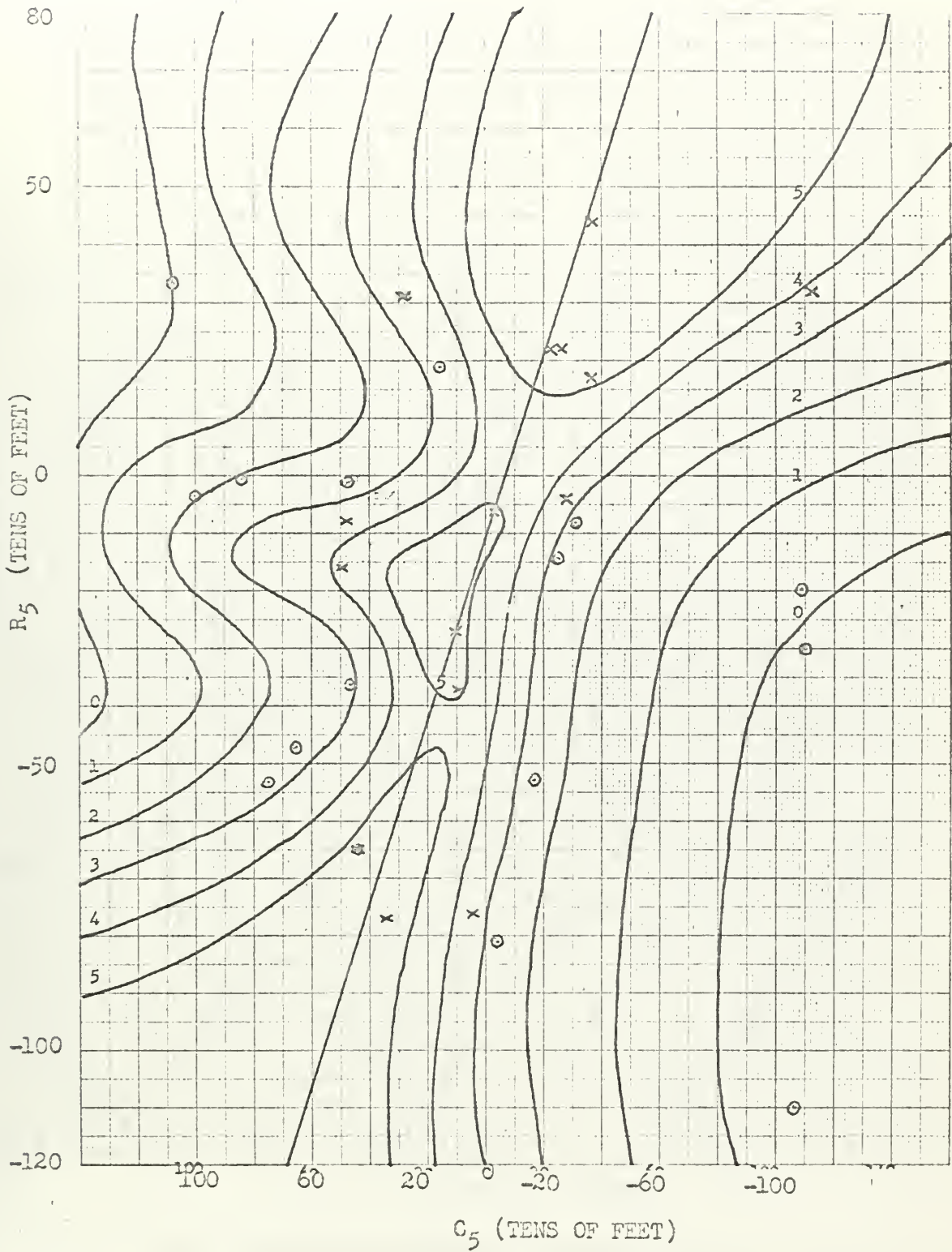


Fig. 6. Graph of relative confidence for C_5R_5 .

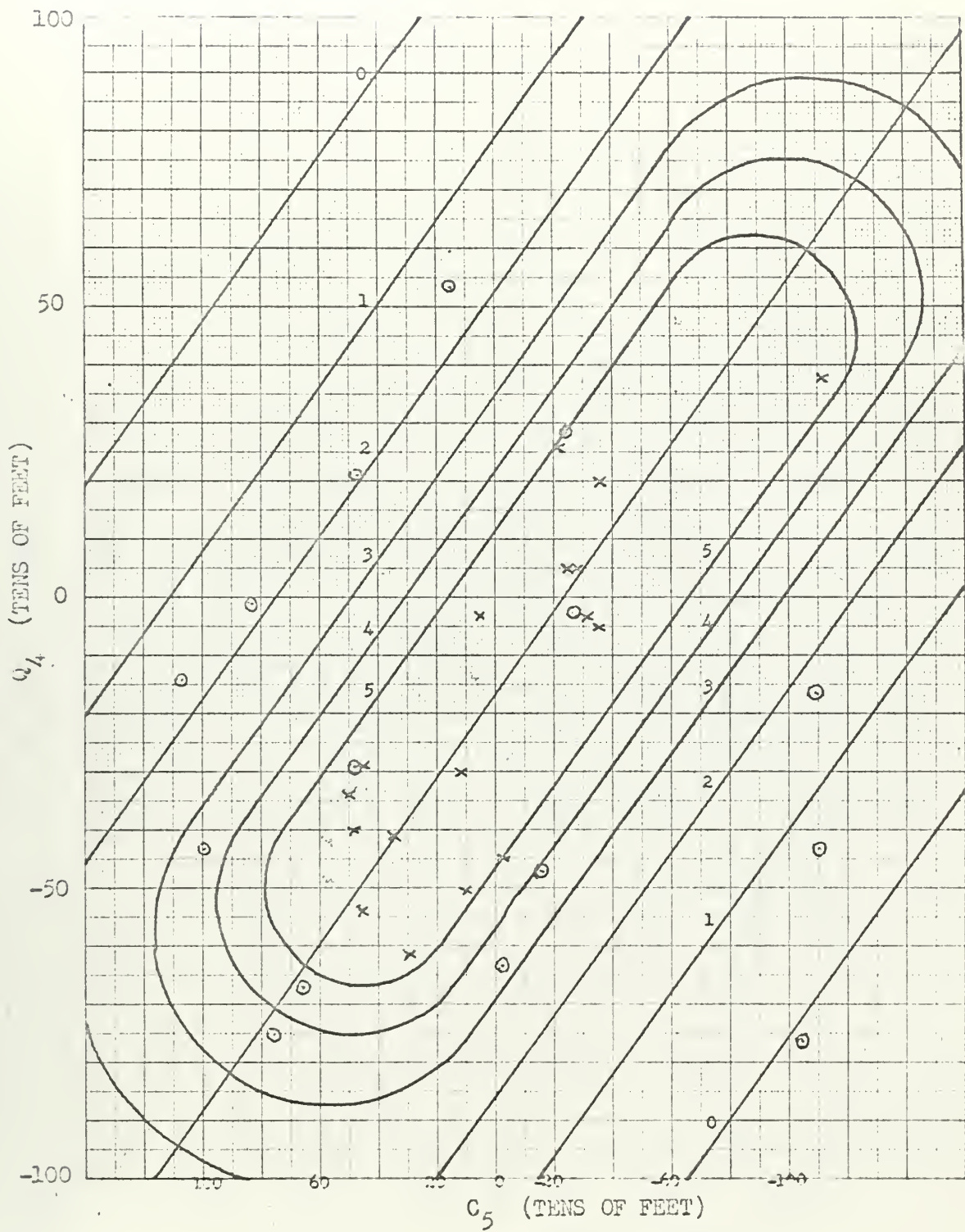


Fig. 7 Graph of relative confidence values for C_5Q_4 .

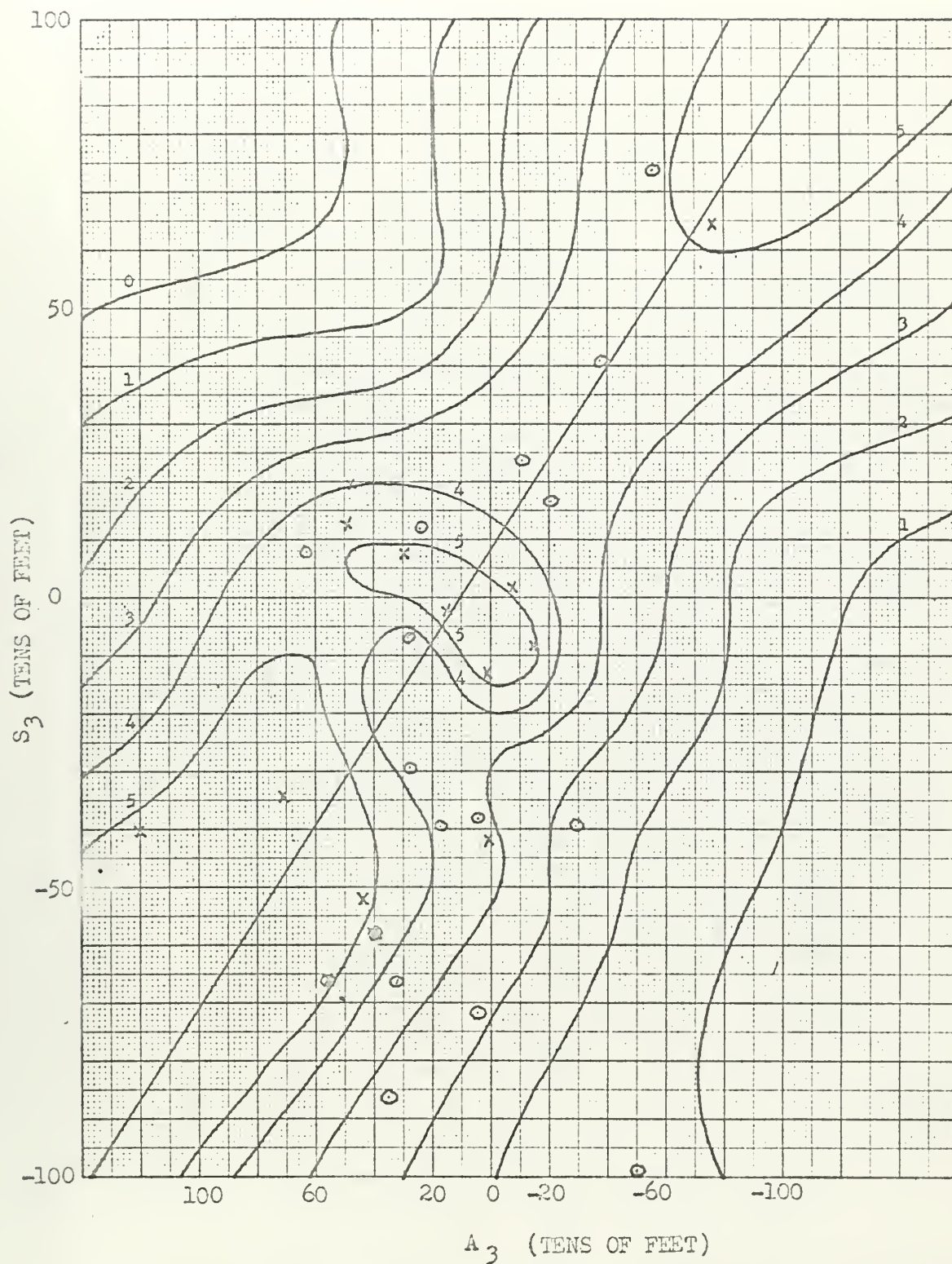


Fig. 8 Graph of relative confidence values for A_3S_3 .

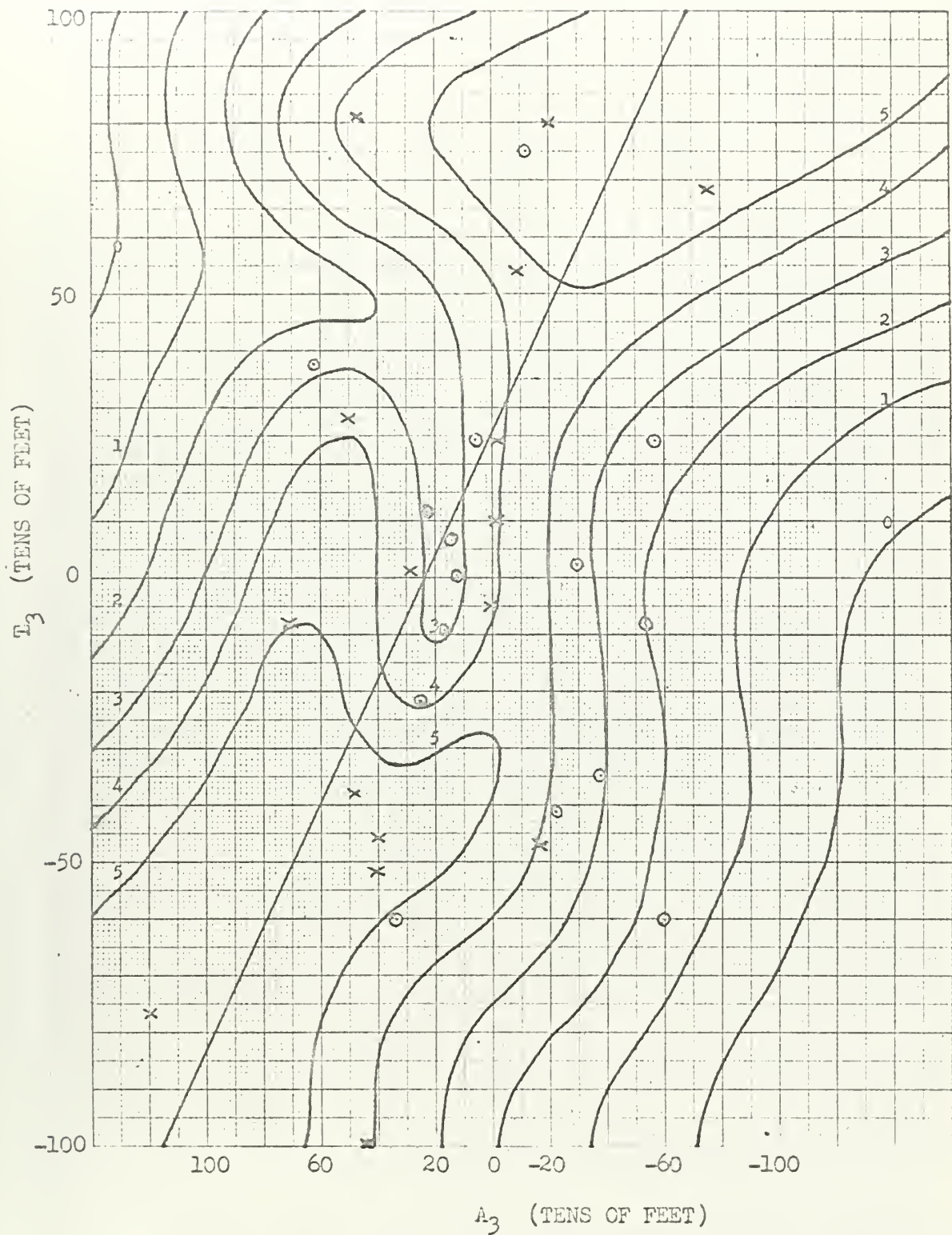


Fig. 9 Graph of relative confidence values for $A_3 T_3$.

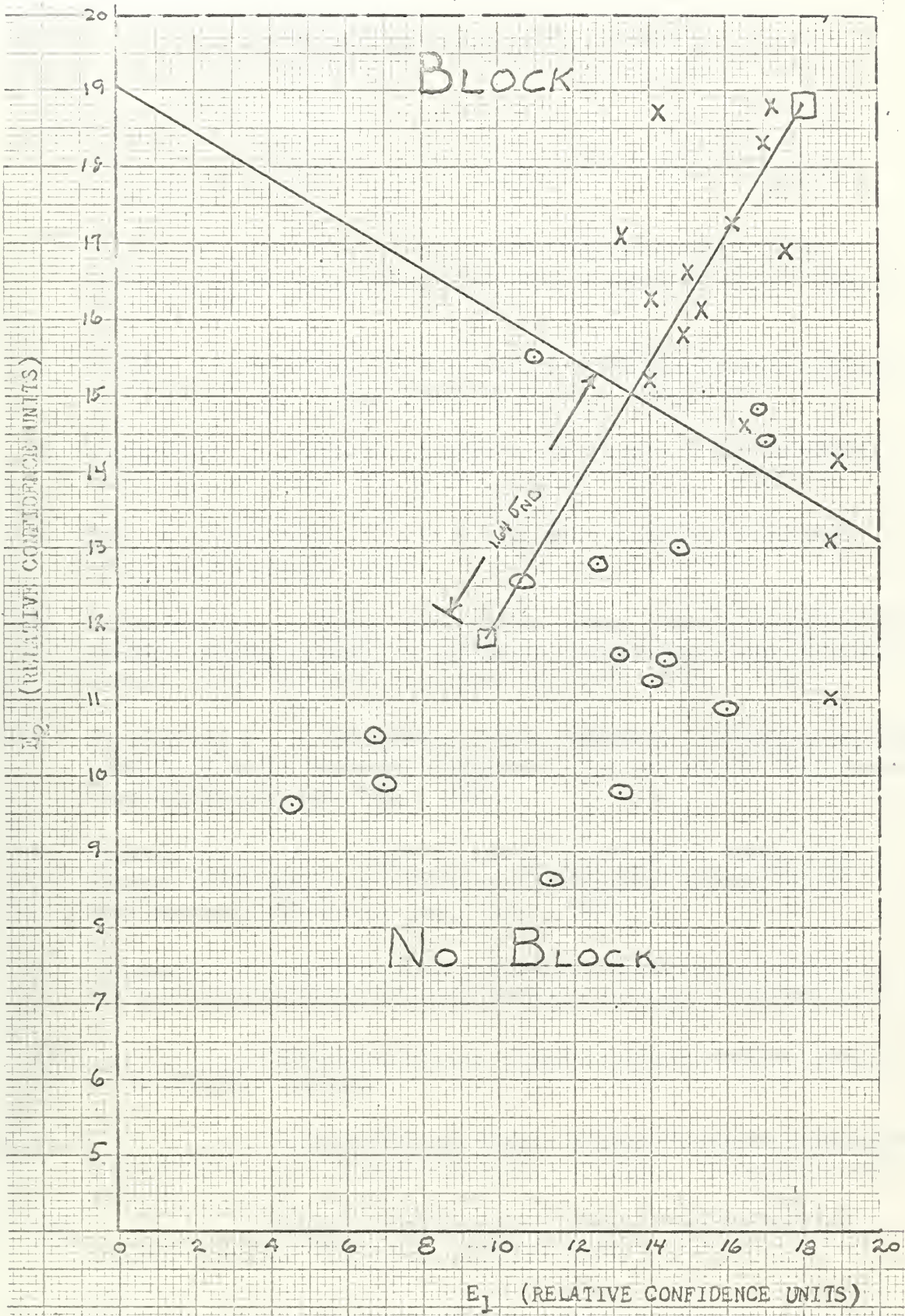


Fig. 10 The forecast graph with E_1 and E_2 given by equations 8 and 9.

BIBLIOGRAPHY

1. Hoel, P. , Introduction to Mathematical Statistics, New York, John Wiley and Sons, 258 pp. , 1956.
2. Elliott, R. , Extended-range forecasting by weather types, Compendium of Meteorology, 834-840, American Meteorological Society, 1951.
3. Miller, R. , Selecting variates for multiple discriminant analysis, The Travelers Weather Research Center, July, 1960.
4. Petterssen, S. , Weather Analysis and Forecasting, Volume II, New York, McGraw-Hill Book Company, 266 pp. , 1956.
5. Rex, D , Blocking action in the middle troposphere and its effect upon regional climate, 196-211, Tellus, 1950.
6. Selfridge, S. , N. Stevenson, and E. Wood, The development of a weather-typing system for extended-range forecasting, Master's Thesis, U. S Naval Postgraduate School, 155 pp. , 1960.
7. Serebreny, S. , E. Wiegman, and R. Hadfield, A study of jet-stream conditions in the Northern Hemisphere during spring, Pan American World Airways, Inc. , 1957.
8. Serebreny, S. , E. Wiegman, and R. Hadfield, A study of jet-stream conditions in the Northern Hemisphere during winter, Pan American World Airways, Inc. , 1957.
9. Thompson, J. , A Numerical method for forecasting rainfall in the Los Angeles area, Monthly Weather Review, 113-124, July, 1950.
10. _____, Historical series of daily synoptic weather maps, U. S. Weather Bureau.
11. _____, Normal 500-mb charts for the Northern Hemisphere, United States Navy Weather Research Facility, November, 1957.
12. _____, Standard Mathematical Tables, Twelfth Edition, Chemical Rubber Company, 237-243, 1959.

APPENDIX I

Height anomalies for 15 cases of

Sub-Icelandic blocks

(Values given in tens of feet)

Case#	A ₆	B ₆	V ₆	C ₅	Q ₅	R ₅	Q ₄	A ₃	S ₃	T ₃
1	-25	+62	-66	-25	+12	+22	+ 5	-76	+65	+68
2	-36	+ 2	+62	+ 5	- 4	-76	- 3	+43	-52	-109
3	-47	-66	+43	- 3	-30	- 6	-45	- 2	+15	+24
4	-31	-72	+77	+11	-45	-27	-30	+29	+ 8	+ 1
5	+81	+40	- 4	+10	- 1	-37	-50	+40	-58	-46
6	+35	+90	-28	+35	-56	-77	-41	+51	-66	+28
7	-20	-80	+57	-22	+17	+22	+26	- 8	+ 2	+54
8	-28	+27	+39	-36	+28	+17	- 5	+48	+20	+81
9	+ 4	+46	+12	+50	- 5	-16	-34	± 0	-41	- 5
10	-53	-77	+36	-28	+74	- 4	+ 5	-16	- 8	-47
11	+32	-16	-12	-36	+80	+44	+20	+49	+13	-38
12	+40	+65	+15	+48	+17	- 8	-40	+71	-34	- 8
13	+30	+86	-77	+45	-29	-65	-54	- 1	-14	+10
14	+31	+69	-11	+29	+ 4	+26	-61	+120	-40	-77
15	-18	-11	-35	-112	+51	+32	+38	+41	- 5	-52

APPENDIX II

Height anomalies for 15 cases of
non-blocks in Sub-Icelandic area

Case #	A ₆	B ₆	V ₆	C ₅	Q ₅	R ₅	Q ₄	A ₃	S ₃	T ₃
1	+14	+45	-11	+47	-1	-1	+21	+32	-66	-59
2	-37	+23	-62	+45	-47	-36	-29	-53	-139	-8
3	-8	+21	+51	-17	-54	-53	-47	+35	-86	-60
4	+22	-35	-79	-110	-17	-20	-16	+15	-39	+6
5	-2	+88	-38	+107	+4	+34	-14	+63	+8	+37
6	+65	+63	+68	+65	+5	-47	-67	±0	-71	+12
7	-24	-36	-15	-25	+18	-14	+29	-56	+74	+24
8	-13	+26	+57	+75	-62	-53	-75	-29	-39	+2
9	-47	±0	-9	+83	-6	±0	-1	-11	+24	+75
10	+4	-9	-35	-3	-69	-81	-63	-38	+41	-35
11	-73	+45	-86	+99	-12	-3	-43	+26	-6	+11
12	-16	+17	-17	-32	-30	-8	-3	+27	-29	-22
13	-95	-48	-68	+15	+19	+19	+54	+20	+11	-10
14	+1	-97	-55	-111	-47	-30	-43	-21	+17	-41
15	-32	-92	+20	-106	-87	-110	-76	+4	-41	+24

APPENDIX III

Test data; height anomalies for 15 block cases

miscellaneous areas

Case #Block Type

- | | |
|-----|---------------------------|
| 1. | Bering Sea-Western Alaska |
| 2. | Sub-Aleutian |
| 3. | Sub-Aleutian |
| 4. | Bering Sea-Western Alaska |
| 5. | England-North Sea |
| 6. | Scandinavian-Baltic |
| 7. | Western Canada |
| 8. | Western Canada |
| 9. | England-North Sea |
| 10. | Bering Sea-Western Alaska |
| 11. | Scandinavian-Baltic |
| 12. | Sub-Icelandic |
| 13. | Scandinavian-Baltic |
| 14. | Sub-Icelandic |
| 15. | Sub-Aleutian |

Case #	Date	Z_{AL}	\bar{Z}_{AL}	z	Z_{BL}	\bar{Z}_{BL}	z_{BL}	Z_{VL}	\bar{Z}_{VL}	z_{VL}
1.	1/5/54	692	768	-76	761	745	+16	795	784	+11
2.	2/4/54	781	779	+2	659	764	-95	752	770	-18
3.	1/8/57	822	787	+35	819	776	+43	737	774	-37
4.	1/13/54	834	783	+51	830	769	+61	710	777	-67
5.	2/22/53	848	779	+69	890	802	+88	640	758	-118
6.	1/23/56	779	779	± 0	798	783	+15	675	778	-103
7.	2/16/50	825	753	+72	800	780	+20	815	780	+35
8.	2/22/57	733	772	-39	740	785	-45	833	775	+58
9.	1/16/54	770	788	-18	818	802	+16	840	760	+80
10.	3/19/56	762	770	-8	729	749	-20	810	793	+17
11.	1/24/57	794	777	+17	775	787	-12	830	773	+57
12.	12/3/45	758	790	-48	805	790	+15	783	730	+53
13.	1/25/51	770	773	-3	798	778	+20	791	781	+10
14.	3/20/57	721	799	-78	738	797	-59	756	740	+16
15.	2/12/57	840	784	+56	824	780	+44	780	772	+8

Case #	Date	Z_{CS}	\bar{Z}_{CS}	z_{CS}	Z_{QS}	\bar{Z}_{QS}	z_{QS}	Z_{RS}	\bar{Z}_{RS}	z_{RS}
1.	1/6/54	688	721	-33	740	703	+37	749	729	+20
2.	2/5/54	692	742	-50	700	690	+10	755	701	+54
3.	1/9/57	810	754	+56	680	690	-10	690	686	+4
4.	1/14/54	799	744	+55	668	685	-17	715	693	+22
5.	2/23/53	840	802	+38	690	729	-39	711	719	-8
6.	1/24/56	781	801	-20	750	760	-10	758	740	+15
7.	2/17/50	781	783	-2	768	742	+26	698	729	-31
8.	2/23/57	703	780	-77	800	742	+58	725	708	+17
9.	1/17/54	872	809	+63	705	731	-26	644	719	-75
10.	3/20/56	729	728	+1	769	732	+37	700	750	-50
11.	1/25/57	815	804	+11	640	748	-109	649	730	-81
12.	12/4/45	785	766	+19	724	721	+3	752	720	+32
13.	1/26/51	770	804	-34	857	767	+90	846	749	+97
14.	3/21/57	759	776	-17	751	751	± 0	770	743	+27
15.	2/13/57	762	770	-8	699	701	-2	716	690	+26

Case #	Date	Z_{Q_4}	\bar{Z}_{Q_4}	Z_{Q_4}
1.	1/7/54	716	703	+13
2.	2/6/54	680	690	-10
3.	1/10/57	660	690	-30
4.	1/15/54	682	685	-3
5.	2/24/53	685	729	-44
6.	1/25/56	750	760	-10
7.	2/18/50	777	742	+35
8.	2/24/57	792	742	+50
9.	1/18/54	648	731	-93
10.	3/21/56	742	732	+10
11.	1/26/57	690	748	-58
12.	12/5/45	741	721	+20
13.	1/27/51	852	767	+85
14.	3/22/57	757	751	+6
15.	2/14/57	671	701	-30

Case #	Date	Z_{R_3}	\bar{Z}_{R_3}	z_{R_3}	Z_{S_3}	\bar{Z}_{S_3}	z_{S_3}	Z_{T_3}	\bar{Z}_{T_3}	z_{T_3}
1.	1/8/54	710	768	-58	760	761	-1	804	780	+24
2.	2/7/54	769	779	-10	772	733	+39	798	768	+30
3.	1/14/57	819	787	+32	701	715	-14	760	761	-1
4.	1/16/54	841	783	+58	723	730	-7	731	770	-39
5.	2/25/53	850	779	+71	730	730	± 0	750	761	-11
6.	1/26/56	761	779	-18	761	718	+43	770	728	+42
7.	2/19/50	812	753	+59	703	701	+2	660	693	-33
8.	2/25/57	809	772	+37	715	690	+25	690	701	-11
9.	1/19/54	817	788	+29	712	721	-9	668	753	-85
10.	3/22/56	688	770	-82	748	780	-32	781	796	-15
11.	1/27/57	804	776	+28	639	719	-80	690	737	-47
12.	12/6/45	820	790	+30	721	733	-12	718	760	-42
13.	1/28/51	792	773	+19	699	720	-21	660	725	-65
14.	3/23/57	779	799	-20	806	754	+52	791	792	-1
15.	2/15/57	870	784	+86	746	695	+51	722	733	-11

APPENDIX IV

Test data; height anomalies for 15 cases of
non-blocks, miscellaneous areas

F-6

Case #	Date	Z _{AG}	\bar{Z}_{AG}	Z _{AG}	Z _{BG}	\bar{Z}_{BG}	Z _{BG}	Z _{VG}	\bar{Z}_{VG}	Z _{VG}
1.	1/10/53	735	768	-33	712	745	-33	721	784	-63
2.	2/1/57	885	779	+106	888	764	+124	800	770	+30
3.	1/11/51	777	787	-10	760	776	-16	780	774	+6
4.	1/25/52	702	783	-81	643	769	-126	792	777	+15
5.	2/5/51	763	779	-16	679	802	-123	782	758	+24
6.	3/8/57	737	788	-51	808	799	+9	734	780	-46
7.	2/19/57	775	753	+22	746	780	-34	821	780	+41
8.	2/22/51	810	772	+38	823	785	+38	744	775	-31
9.	1/10/52	733	788	-55	785	802	-17	873	760	+113
10.	3/14/57	812	770	+42	700	749	-49	843	793	+50
11.	1/1/51	740	776	-36	729	787	-58	798	773	+25
12.	2/19/51	705	782	-77	701	786	-85	658	733	-75
13.	1/8/53	805	773	+32	779	778	+1	690	781	-91
14.	3/1/54	708	799	-91	803	797	+6	688	740	-52
15.	2/16/51	817	784	+33	760	780	-20	811	772	+29

F-5

Case #	Date	Z_{C5}	\bar{Z}_{C5}	z_{C5}	Z_{Q5}	\bar{Z}_{Q5}	z_{Q5}	Z_{R5}	\bar{Z}_{R5}	z_{R5}
1.	1/11/53	728	721	+7	680	703	-23	680	729	-49
2.	2/2/57	872	742	+130	712	690	+22	741	701	+40
3.	1/12/51	712	754	-42	658	690	-32	636	686	-50
4.	1/26/52	692	744	-52	685	685	± 0	690	693	-3
5.	2/6/51	741	802	-61	710	729	-19	740	719	+21
6.	3/9/57	840	809	+31	790	768	+22	822	752	+70
7.	2/20/57	803	783	+20	696	742	-46	680	729	-49
8.	2/23/51	840	780	+60	801	742	+59	740	708	+38
9.	1/11/52	804	809	-5	757	731	+26	762	719	+43
10.	3/15/57	635	728	-93	758	732	+26	777	750	+27
11.	1/2/51	720	804	+84	745	748	-3	767	730	+37
12.	2/20/51	792	761	+31	795	718	+77	773	716	+57
13.	1/9/53	800	804	-4	691	767	-76	700	749	-49
14.	3/2/54	858	776	+82	769	750	+19	759	743	+16
15.	2/17/51	798	770	+28	702	701	-1	675	690	-15

Case #	Date	Z_{Q4}	\bar{Z}_{Q4}	Z_{Q4}
1.	1/12/53	642	703	- 61
2.	2/3/57	756	690	+ 66
3.	1/13/51	640	690	- 50
4.	1/27/52	690	685	+ 5
5.	2/7/51	800	729	+ 71
6.	3/10/57	810	768	+ 52
7.	2/21/57	763	742	+ 21
8.	2/24/51	752	742	+ 10
9.	1/12/52	796	731	+ 65
10.	3/16/57	726	732	- 6
11.	1/3/51	775	748	+ 27
12.	2/21/51	760	718	+ 42
13.	1/10/53	740	767	- 27
14.	3/3/54	709	750	- 41
15.	2/18/51	701	701	\pm 0

Case #	Date	Z_{A_3}	\bar{Z}_{A_3}	z_{A_3}	Z_{S_3}	\bar{Z}_{S_3}	z_{S_3}	Z_{T_3}	\bar{Z}_{T_3}	z_{T_3}
1.	1/13/53	704	768	- 64	760	761	-1	810	780	+ 30
2.	2/4/57	839	779	+ 60	730	733	- 3	711	768	-57
3.	1/14/51	731	787	- 56	750	715	+ 35	761	761	± 0
4.	1/28/52	726	783	- 57	681	730	-49	770	770	± 0
5.	2/8/51	795	779	+ 16	641	730	- 91	762	761	+ 1
6.	3/11/57	820	788	+ 32	772	744	+28	740	753	- 13
7.	2/22/57	768	753	+ 15	698	701	- 3	669	693	- 30
8.	2/25/51	751	772	- 21	720	690	+ 30	720	701	+19
9.	1/13/52	841	788	+ 53	746	721	+25	757	753	+ 4
10.	3/17/57	736	770	- 34	800	780	+ 20	772	796	- 24
11.	1/4/51	824	776	+ 48	703	719	- 16	701	737	- 36
12.	2/22/51	726	782	- 56	782	727	+ 55	812	765	+ 47
13.	1/11/53	775	773	+ 2	801	720	+ 81	720	725	- 5
14.	3/4/54	677	799	- 122	772	754	+ 18	829	792	+ 37
15.	2/19/51	763	784	- 21	722	695	+ 27	740	733	+ 13

thesH88

A method of forecasting the formation of



3 2768 002 13238 3

DUDLEY KNOX LIBRARY